

NASA TECHNICAL NOTE

NASA TN D-8204



NASA TN D-8204

p.1

LOAN COPY: RI
AFWL TECHNICAL
KIRTLAND AFB

0133763

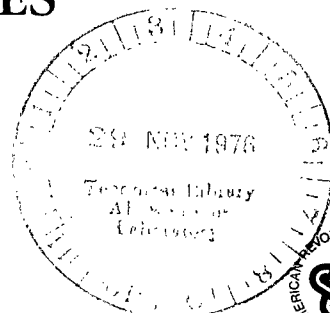


EFFECT OF FIBER DIAMETER AND MATRIX ALLOYS ON IMPACT-RESISTANT BORON /ALUMINUM COMPOSITES

David L. McDanel and Robert A. Signorelli

Lewis Research Center

Cleveland, Ohio 44135





0133763

1. Report No. NASA TN D-8204	2. Government Accession No.	3. Recipient's Catalog No.	
4. Title and Subtitle EFFECT OF FIBER DIAMETER AND MATRIX ALLOYS ON IMPACT-RESISTANT BORON/ALUMINUM COMPOSITES		5. Report Date November 1976	6. Performing Organization Code
7. Author(s) David L. McDanel and Robert A. Signorelli	8. Performing Organization Report No. E-8648		10. Work Unit No. 505-01
9. Performing Organization Name and Address Lewis Research Center National Aeronautics and Space Administration Cleveland, Ohio 44135		11. Contract or Grant No.	
12. Sponsoring Agency Name and Address National Aeronautics and Space Administration Washington, D.C. 20546		13. Type of Report and Period Covered Technical Note	
15. Supplementary Notes		14. Sponsoring Agency Code	
16. Abstract <p>Efforts to improve the impact resistance of B/Al are reviewed and analyzed. Nonstandard thin-sheet Charpy and Izod impact tests and standard full-size Charpy impact tests were conducted on composites containing unidirectional 0.10-, 0.14-, and 0.20-mm-(4-, 5.6-, and 8-mil-) diameter boron fibers in 1100, 2024, 5052, and 6061 Al matrices. Impact failure modes of B/Al are proposed in an attempt to describe the mechanisms involved and to provide insight for maximizing impact resistance. The impact strength of B/Al was significantly increased by proper selection of materials and processing. The use of a ductile matrix (1100 Al) and large-diameter (8-mil) boron fibers gave the highest impact strengths. This combination resulted in improved energy absorption through matrix shear deformation and multiple fiber breakage.</p>			
17. Key Words (Suggested by Author(s)) Composite materials; Impact tests Charpy impact test; Compressor blades Boron; Aluminum; Metal matrix composites		18. Distribution Statement Unclassified - unlimited STAR category 24	
19. Security Classif. (of this report) Unclassified	20. Security Classif. (of this page) Unclassified	21. No. of Pages 37	22. Price* \$4.00

EFFECT OF FIBER DIAMETER AND MATRIX ALLOYS ON IMPACT-RESISTANT BORON/ALUMINUM COMPOSITES

by David L. McDanel and Robert A. Signorelli

Lewis Research Center

SUMMARY

Efforts to improve the impact resistance of boron/aluminum (B/Al) composites are reviewed and analyzed. Nonstandard thin-sheet Charpy and Izod impact tests and standard full-size Charpy impact tests were conducted at room temperature on composites containing unidirectional 0.10-, 0.14-, and 0.20-mm- (4-, 5.6-, and 8-mil-) diameter boron fibers in 1100, 2024, 5052, and 6061 Al matrices. Impact failure modes of B/Al are proposed in an attempt to describe the mechanisms involved and to maximize impact resistance.

The impact strength of B/Al was significantly increased by proper selection of materials and processing. The use of a ductile matrix (1100 Al) and large-diameter (8-mil) boron fibers gave the highest impact strengths. This combination resulted in improved energy absorption through matrix shear deformation and multiple fiber breakage. The large-diameter boron fibers provide larger interfiber spacings, which in turn allow the matrix to deform in a ductile manner that permits the fibers to attain a greater portion of their full strength and strain.

There is an optimum fabrication temperature for B/Al. Processing below this temperature resulted in delamination upon impact at lower energies. Composites fabricated at the optimum temperature absorbed energy by matrix shear and fiber fracture. Fabrication above the optimum temperature reduced the impact strength by strength and ductility degradations caused by fiber/matrix interfacial reaction.

INTRODUCTION

Studies by NASA and the Air Force have shown the advantages of using composites as rotating fan and compressor blades in aircraft turbine engines. Compos-

ites offer lighter weight, lower cost, and higher specific strength and stiffness, resulting in improved engine performance and lower direct operating costs (ref. 1). Some of the advantages of using various metal-matrix composites in different areas of aircraft gas turbine engines are discussed in reference 2. Increases in impact resistance are reported for fans and compressors. Increases in use-temperatures are reported for the turbine section.

Most prior materials development has been directed toward using the high specific strength and stiffness of composites for airframe structures. High mechanical properties are most important for these applications, and little attention has been given to impact resistance. However, for rotating fan and compressor blades in aircraft engine applications, impact and foreign-object-damage (FOD) resistance become as important to operational performance as strength and stiffness. Reference 3 defines an FOD spectrum as small-body and large-body damage. Small-body damage includes hard objects such as sand, rocks, rivets, and ice balls. Large-body FOD is caused by hard bodies, such as ice slabs, and soft bodies, such as birds. Localized damage from small-body impact can result in a minor reduction in fatigue strength. Large-body impact can cause complete airfoil separation, requiring a reduction in engine speed or complete shutdown.

Collisions with birds are a major flight safety hazard encountered in aircraft operation. Most collisions are with birds ranging in weight from 110-gram (4-oz) starlings to 1.8-kilogram (4-lb) ducks. During the 1967-69 period, 35 percent of all aircraft accidents were attributable to bird strikes (ref. 4). As shown in figure 1, 52 percent of the bird population is found at altitudes less than 152.5 meters (500 ft), where they endanger takeoff and landing operations. Although FAA regulations require that an aircraft must be able to take off with one engine not operating, takeoff conditions are the most severe as the engines are required to operate at full power and the loss or reduction of power could be catastrophic. Normally, bird strikes are rare above 457.5 meters (1500 ft), but during migration periods the highest bird population density occurs in the 457.5- to 610-meter (1500- to 2500-ft) altitude range. Bird strikes are less critical for subsonic aircraft at higher altitudes because the engines are under reduced cruise power.

Lack of FOD resistance has been a major obstacle to the use of composites as fan blades in aircraft engines. Although composite blades have shown considerable promise in preliminary testing, in full-stage engine tests, the results have been

less than satisfactory. The results indicate that composite blades must have additional impact resistance to become competitive with conventional titanium and stainless steel blades. In addition, root attachment methods used for the blades have caused fiber breakage during fabrication, resulting in premature failure during engine operation.

To overcome these problems, the NASA Lewis Research Center has conducted studies to improve the impact resistance of both polymer- and metal-matrix composites for fan blade applications. This report reviews the programs supporting the impact improvement of unidirectional B/Al composites and analyzes some of the factors that can increase the impact resistance of metal-matrix composites. Room-temperature tensile and dynamic modulus-of-elasticity tests, thin-sheet Izod and Charpy impact tests, and full-size Charpy tests were conducted to determine the effect of processing variables, matrices, and boron fiber diameter on the impact resistance of B/Al composites. Impact failure modes are proposed and are related to the results obtained.

MATERIALS AND PROCEDURE

Materials Selection

Commercially produced boron fiber, 0.10, 0.14, and 0.20 mm (4, 5.6, and 8 mils) in diameter, was used for composites in this investigation. Because of the standard nomenclature used in the aerospace industry, the boron fiber diameter will be referred to in mils, rather than in SI units, throughout the remainder of this report.

Aluminum alloy matrices, 1100, 2024, 5052, and 6061, were selected to cover a wide range of impact strengths and ductilities. Properties of the matrix alloys selected are shown in table I (ref. 5).

Specimen Preparation

All B/Al panels for the in-house program were produced by Avco Corp. and nominally contained 48-volume-percent boron. They were made by press diffusion bonding in vacuum. The first series of panels, consisting of eight-ply unidirectional 8-mil-diameter-B/1100 Al composites, were used to determine the effect of fabrication temperature on impact properties. These panels were fabricated at temperatures

from 714 to 783 K (825^o to 950^o F) and at a pressure of 34 MPa (5 ksi), which was in the range normally used by other fabricators.

After a standard fabrication condition, 755 K (900^o F) for 0.5 hour at 34 MPa (5 ksi), was selected, another series of 1100 Al matrix panels were fabricated. In addition, panels of 2024 Al were fabricated at 774 K (935^o F) and panels of 6061 Al and 5052 Al were fabricated at 805 K (965^o F), for 0.5 hour at 34 MPa (5 ksi). The eight-ply panels, used for tensile and thin-sheet impact specimens, were 30.5 cm x 30.5 cm (12 in. x 12 in.) square and 0.20 cm (0.080 in.) thick for the 8-mil-diameter-boron panels, 0.15 cm (0.060 in.) thick for the 5.6-mil panels, and 0.10 cm (0.040 in.) thick for the 4-mil panels. Panels for full-size Charpy specimens were 15 cm x 15 cm x 1 cm (6 in. x 6 in. x 0.4 in.) and contained 40 plies for the 8-mil-diameter-boron panels, while the 5.6-mil panels were 60 ply, and the 4-mil panels were 80 ply.

Specimen Geometry

Because of the anisotropic properties of composites, specimen geometry must be uniquely defined in terms of fiber direction, pressing direction, and notch location. These geometries are shown in figure 2. The LT, TT, and TL geometries are defined in references 6 and 7. The LT geometry is further defined in reference 8 as LT, where the notch is in a plane normal to the pressing direction, and LT(s), where the notch is on a side parallel to the pressing direction. Tests were conducted on specimens with LT, LT(s), and TT geometries for the studies reported herein.

Impact Tests

Three types of pendulum impact tests were conducted: unnotched thin-sheet Izod, unnotched thin-sheet Charpy, and notched full-size Charpy. All impact tests were conducted at room temperature. Thin-sheet tests were conducted because they are more economical in terms of material and machining costs and serve as a convenient screening technique. The cantilever mounting of the thin-sheet Izod test tends to simulate the behavior of a modern, thin-airfoil fan blade in engine operation. Thin-sheet Charpy tests provided an indication of the unrestrained behavior of the

material. Full-size Charpy test results provided a comparison of standard specimens with literature values of other materials.

Thin-sheet Izod tests were conducted on a Bell Telephone Laboratories miniature Izod impact testing machine. With appropriate weights on the tup the capacity was 7.0 J (61.8 in-lb). The calibration and operation of this machine are described in reference 9. Nonstandard unnotched specimens were 3.8 cm x 0.64 cm (1.5 in. x 0.25 in.).

Thin-sheet Charpy tests were conducted on a TMI low-capacity impact testing machine with the grips modified to give standard ASTM separation. The tup used had a maximum capacity of 5.4 J (4 ft-lb). Nonstandard unnotched specimens were 5.6 cm x 1.0 cm (2.2 in. x 0.4 in.).

Full-size Charpy impact tests were conducted on a Rheile impact testing machine with a capacity of 163 J (120 ft-lb). Tests and specimens were made according to ASTM standard E23-66 (ref. 10). Some specimens were slightly undersize (up to 0.25 mm) in thickness. In these cases the notch was undercut so that the remaining material under the notch met the ASTM standard.

Tensile Tests

Room-temperature tensile tests were conducted on an Instron screw-driven-crosshead universal testing machine. A strain-gage extensometer with a 2.54-cm (1-in.) gage length was used to measure strain with an X-Y recorder. A crosshead speed of 0.025 cm/min (0.01 in/min) was used at the start of the test to measure initial elastic strain. The crosshead speed was increased to 0.25 cm/min (0.1 in/min) after the test was underway.

Two specimen geometries were used. Longitudinal specimens (testing direction parallel to fiber axis) were 13 cm x 0.95 cm (5 in. x 0.375 in.). Aluminum doublers, 4.75 cm (1.88 in.) long were adhesively bonded to the ends of the sheet specimens, leaving a gage length of 3.2 cm (1.25 in.). Transverse specimens (testing direction perpendicular to fiber axis) were 7.6 cm x 0.95 cm (3 cm x 0.375 in.). Doublers for these specimens were slightly under 2.5 cm (1 in.) long.

Dynamic Modulus-of-Elasticity Tests

The room-temperature dynamic modulus of elasticity of B/Al composites was measured by sonic methods. Specimens were 13 cm x 0.95 cm (5 in. x 0.375 in.). Modulus was determined by measuring the resonant frequency of the fundamental flexural mode of vibration. Resonance was determined from maximum oscilloscope and voltmeter deflections from stereo phonograph cartridges placed on each end of the specimen. Resonance was verified to be fundamental flexural vibration by moving the receiving cartridge along the length of the specimen and observing the nodal points and the change in the oscilloscope ellipse angle. The dynamic modulus was calculated by using equations from reference 11, based upon reference 12.

RESULTS

Fabrication-Condition Screening Tests

Room-temperature, thin-sheet Izod impact screening tests were conducted on 8-mil-diameter-B/1100 Al composites to determine the effect of fabrication temperature on impact properties. Results of these tests are presented in table II, and typical failed specimens are shown in figure 3. Impact strengths are area compensated to kilojoules per square meter and foot-pounds per square inch.

Longitudinal specimens fabricated at lower temperatures failed by delamination at low impact energies. Delamination occurred along the fiber/matrix interface, and no aluminum was visible along the fiber (fig. 4). After fabrication at 741 K (875^o F) for 1 hour, or at 755 K (900^o F) for 0.5 hour, the failure underwent a transition to a fibrous failure with no delamination. At higher bonding temperatures the impact strength decreased slightly, but the specimens did not delaminate. Based on these impact results, as well as on the ability to resist delamination during machining, a standard fabrication condition of 755 K (900^o F) at 34 MPa (5 ksi) for 0.5 hour was chosen for the remainder of the 1100 Al matrix specimens.

Specimens tested in the transverse direction failed at low impact energies by brittle separation into two pieces. It appeared that processing at higher temperatures increased the transverse impact strength slightly.

Dynamic Modulus-of-Elasticity Tests

Room-temperature dynamic modulus tests were conducted on composites of various boron fiber diameters and aluminum matrix alloys. Results of tests in the longitudinal and transverse directions are presented in table III. The modulus was independent of fiber diameter and matrix alloy.

Tensile Tests

Ultimate tensile strength results are presented in table IV. Longitudinal strengths of 1100-Al-matrix composites were lower with 8-mil-diameter boron fibers than with the 5.6- and 4-mil-diameter fibers. Stress-strain curves of all specimens were similar and showed linear behavior to failure. The 6061-Al-matrix composites were the strongest, and the 5052 Al was slightly weaker than the 1100 Al. The strength of the 2024-Al-matrix composites was the lowest of all. The 2024-Al-matrix specimens seemed to be well bonded, so no explanation can be given for this reduced strength.

Results of transverse tensile tests are also presented in table IV. Tests on 1100-Al-matrix composites indicated no change in transverse strength with fiber diameter. The strength of specimens with 4-mil-diameter boron fibers was not determined because the specimens broke while being loaded. The transverse strengths of the higher-strength-matrix composites were about twice that of the 1100-Al-matrix composite.

Impact Tests

Thin-sheet Izod impact test results are presented in table V, thin-sheet Charpy results in table VI, and full-size Charpy results in table VII. Results of full-size Charpy tests from reference 8 are also included in table VII.

Figure 5 compares the area-compensated LT impact strength of unidirectional 1100-Al-matrix composites for three different fiber diameters. The area under the notch was used to compensate area for full-size Charpy specimens. Thin-sheet specimens were unnotched, and the entire cross section was used for measurement. For each type of test the area-compensated impact strength increased with increasing fiber diameter. The values for full-size Charpy tests of 8-mil-diameter boron-

fiber specimens are shown as a band because the panels used for the Lewis in-house tests were inadequately bonded and failed at excessively low energies. Therefore, the lower bound represents an extrapolation from angleply test results (ref. 13). The upper bound represents impact values from reference 8. In either case the increase in impact strength from 5.6- to 8-mil-diameter-boron-fiber specimens is much greater in full-size Charpy tests than in thin-sheet tests. The impact strength of the 1100-Al-matrix composites was higher than that of the other Al matrices tested.

The area-compensated, full-size Charpy impact strength was much higher than that of thin-sheet specimens. In properly bonded specimens, failure occurred by fracture of all the fibers in the cross section, with matrix plastic shear prior to fiber failure. Full-size Charpy specimens exhibited more shear than thin-sheet specimens. Although the thicknesses of the thin-sheet specimens with each diameter fiber were different, the trends were the same for all types of tests, including the full-size Charpy.

The results obtained indicate that thin-sheet impact tests can be used as a screening tool to rank impact behavior of various B/Al composites. The rankings were consistent for tests on different matrices and fiber diameters. Although the specimen thicknesses and the failure mechanisms varied, the results are still consistent for ranking purposes, but extrapolation of impact strength values from one test to another cannot be made.

DISCUSSION

Measurement of Fracture Energy

One of the problems inherent in composite toughness evaluation is that a variety of testing methods have been used. Interpretation of the behavior is different depending upon whether notched tensile tests or bending/impact tests are conducted. The ends are rigidly restrained in tensile tests; but in slow bend or impact tests, both ends may be free (Charpy) or one end may be clamped (Izod). Although strength in bending should be comparable to strength in tension, the strain behavior is different. Therefore, interpretation of results should be approached with caution when comparing fracture toughness, work of fracture, or impact strength results from different types of tests.

Notched Charpy and Izod impact tests are accepted as convenient methods of

determining the susceptibility of a material to brittle fracture at high strain rates. Although data from these tests have been used with some success, the approach has been largely empirical (ref. 14). For homogeneous materials the effects of notch geometry and elastic and plastic deformation under plane stress and plane strain conditions at both the notch region and throughout the specimen are very complex. The stress state and toughness behavior of composites are even more complex because of the divergent properties of the two constituents.

The difference in area-compensated impact strengths of thin-sheet and full-size impact specimens is related to their thickness and failure mechanisms. References 15 to 17 report a transition in fracture and delamination behavior at a thickness of 0.25 cm (0.1 in.). Below this thickness, plane stress conditions applied and delamination stresses were very high. Fiber/matrix bond failure occurred because of shear stress concentration at the notch tip. Above this thickness, plane strain conditions applied, where transverse tensile stresses at the notch tip caused fiber/matrix bond failure at lower stresses; and the stress to cause delamination remained constant. In both cases the remaining section was notch insensitive after the notched section delaminated and failed as if a notch had not been present (ref. 15).

Reference 18 states that two different concepts can be used to measure fracture energy. One involves measurement of the total energy introduced during fracture, averaged over the entire fracture process. This category includes work of fracture and Charpy impact testing. The other involves measurement of the initial rate of strain-energy release at failure and includes fracture mechanics analyses of fracture initiation. Results on carbon-fiber reinforced glass (ref. 18) showed that work of fracture, which included fiber failure and fiber pullout, was much larger than the energy required to initiate fracture.

An empirical relation to predict impact properties of composites was presented in references 6 and 7. Good agreement was reported in the prediction that impact strength of B/Al may be increased by increasing the tensile strength, volume percentage, and diameter of the fiber and by decreasing the shear strength of the matrix. This relation is valid for predicting general trends but is probably not valid for exact calculation. The apparent agreement noted in references 6 and 7 may be coincidental.

Results from the Lewis programs show that the impact energy of B/Al composites

also depends upon other factors, which are related to fabrication conditions and failure mechanism. This dependence is predicted in reference 19, where impact energy density (strain energy divided by volume) is shown to be influenced by a complex correlation coefficient based upon fabrication-dependent constituent properties.

Relation of Fracture Mode to Impact Energy Absorption

References 20 and 21 report that the work of fracture of a composite is influenced by the strength and fracture behavior of the fiber, the matrix, and the interface between the two. Contributions to energy absorption by each are interrelated and can limit or enhance the contributions of the others.

Table VIII summarizes the relation of fracture mode to impact energy absorption. Cleavage failures would give the lowest energy absorption. Although not encountered in this program, cleavage failure could occur in overbonded composites where interfacial reaction has forced the fiber to lose its identity. Failure would occur in a manner similar to that of brittle homogeneous materials. A planar fracture would have slightly higher energy absorption. In planar fractures, energy absorption would be primarily controlled by the fiber fracture energy with a small matrix contribution. Delamination or fiber pullout failures would have medium impact energy absorption. In delamination failures, energy is absorbed by surface energy release at the B/Al or Al/Al interfaces. With fiber pullout failures, energy is absorbed through frictional sliding and plastic shear at the interface. Failure by matrix shear with a single failure of each fiber gives high energy absorption because each component makes a contribution to the energy absorbed by the composite. The fiber contribution comes from fiber fracture energy, while the matrix and interface contributions are by shear displacement energy. Matrix shear with multiple fiber breakage gives the highest impact energy absorption. In this case each fiber absorbs additional energy because of multiple fracturing, and the matrix contribution is increased because of the additional plastic shear allowed.

While the table indicates the relation of fracture mode to impact energy absorption, it does not indicate how the toughness of composites can be improved. In this report the materials and processing variables that can increase composite toughness by exploitation of these fracture modes are discussed.

Effect of Fabrication Temperature

Impact resistance of B/Al can be increased by using fabrication temperatures that will provide adequate bonding (to prevent delamination and make failure dependent upon fiber fracture energy) so as to obtain the properties required for a given application. At the same time the temperature must be low enough to prevent excessive aluminum boride formation (so that the fibers can exhibit their maximum strain to failure).

Area-compensated Izod impact strength is plotted in figure 6 for thin-sheet specimens bonded for 0.5 hour at various temperatures. Two curves are plotted on this figure: one for delamination failure at the B/Al interfaces, and one for fibrous fracture where the specimen failed as a unit. For delamination failures, impact strength increased with increasing temperature because of improved bonding. Fibrous failures did not occur at lower bonding temperatures. Where fibrous failures occurred, impact strength decreased with increasing temperature. These two curves indicate that the maximum impact strength is obtained at the lowest bonding temperature where delamination will not occur.

Specimens fabricated at lower temperatures failed by delamination at low area-compensated Izod impact strengths. Bonding was not adequate at these temperatures and did not allow the composites to attain their full impact strength. The fiber/matrix interface was weak, and some specimens delaminated upon machining prior to testing.

At higher bonding temperatures the area-compensated thin-sheet Izod impact strength increased. With adequate bonding the stress to cause delamination at the fiber/matrix interface increased, and the matrix could undergo sufficient shear deformation to fracture the fibers. Thus, for optimum impact resistance the failure mechanism changed from being an interface-controlled delamination to being fiber-fracture controlled.

The maximum impact strength obtained for B/1100 Al was in the 741 to 755 K (875^o to 900^o F) range in Lewis in-house tests. Reference 8 reports that the maximum impact strength for their fabrication cycle was obtained at 727 K (850^o F). Thus, there is probably a range over which maximum impact resistance can be obtained. This range would be dependent upon the complete fabrication cycle used and upon the foil surface condition and the amount of deformation present.

With current bonding practice, there probably would be a slight decrease in

ultimate tensile strength at the lower bonding temperatures used to maximize impact strength. This decrease in strength results from the practice of potential overbonding to ensure material reliability. There is a corresponding sacrifice in impact strength because of the increased variation in strain to failure. These bonding deficiencies could be compensated for, although with some difficulty, by better selection of surface preparation, fiber spacing, foil thickness, and pressure.

After fabrication at temperatures in excess of 783 K (950⁰ F), impact strength would probably drop further as a result of fiber degradation from fiber/matrix interfacial reaction. The formation of a thin brittle aluminum boride layer at the interface reduces the strain capability of the fiber, thus reducing tensile strength and impact resistance.

Although impact data were not obtained above 783 K (950⁰ F), property degradation has been observed after processing at higher temperatures. The fatigue limit of B/6061 Al composites was reduced by increasing fabrication temperature (ref. 22). Reference 23 reports a 20 percent increase in full-size Charpy impact strength of silicon-carbide-coated boron (B/SiC)/6061 Al composites to 9.4 J (7.0 ft-lb) by reducing bonding temperature from 838 K (1050⁰ F) to 723 K (842⁰ F).

Effect of Matrix

The purpose of a matrix is to provide sufficient ductility to permit the fibers to attain their full strength during the impact process. With sufficient matrix ductility the fibers more nearly approach their full strain capability; and failure can occur in an optimum manner, where the matrix and the fiber make a full contribution to fracture energy.

In these studies, 8-mil-diameter boron fibers were used to reinforce four aluminum alloy matrices: 1100, 2024, 5052, and 6061. These alloys were chosen to cover a range of impact strengths, tensile strengths, shear strengths, and ductilities. Shear strength of the matrix becomes important only if it is lower than that of the fiber/matrix interface. Reference 24 shows that the B/Al interfacial bond strength in (B/SiC)/1100 Al is greater than the matrix shear strength and that impact failure occurred in the matrix.

Reference 25 proposes that, for matrices where the failure strain is higher than that of the fibers, a crack will propagate by sequential failure of the fibers, followed

by failure of the matrix along a line joining adjacent fiber breaks. If there is a flaw-dependent length-strength effect (ref. 26), where fibers break at different stresses, fiber fractures will not be aligned and there will be regions of matrix shear between fiber failures. This situation is shown schematically in figure 7(a). Analytically predicting work of fracture for this case is difficult because of problems in determining the total area that is undergoing shear. If the strengths of the fibers are uniform and they do not have flaws distributed along their length, the fracture will be nearly planar and the crack will not be deflected from a path directly across the specimen. This would be the case for plastically deforming fibers with uniform properties, such as ductile tungsten wire. Under these conditions no fiber pullout would occur, and work of fracture would be determined by contributions from plastic deformation of the components. In the case of brittle fibers, such as carbon or boron, fracture is initiated by sequential failure of the brittle fibers on a plane normal to the tensile axis. Reference 25 states that fracture of brittle fibers should absorb little energy and that the plastic deformation of matrix bridges connecting fiber lengths on either side of the incipient fracture will determine the work of fracture.

For matrices where the failure strain is lower than that of the fibers, failure will be initiated by the growth of a crack in the matrix (ref. 25). This crack will tend to be planar, and unbroken fibers will be left bridging the crack. These fibers will fail eventually at weak points adjacent to the plane of the matrix crack. The matrix fracture surface will be smooth, with some surface depressions and projecting pulled-out fibers. This situation is shown in figure 7(b). In this case, work of fracture can be predicted by using the analysis of reference 26.

References 20 and 25 to 28 report that maximum work of fracture occurs with discontinuous fiber composites. When a crack propagates through a composite, fibers shorter than the critical length will be pulled out from the matrix rather than broken. Fibers of the critical length will have a maximum pullout distance. Fibers longer than the critical length will fail in tension, normally at a lower work of fracture. Work of fracture is a combination of the work to debond the fibers from the matrix and the work done in pulling the fibers out of the matrix. However, it should be emphasized that this occurs primarily in the case where the matrix is more brittle than the fibers (ref. 25).

For the case where the fiber is ductile and the matrix is very brittle, fracture would be initiated in the brittle matrix. Multiple cracking of the matrix would occur

because deformation is not limited to the plane of final fracture .

The results obtained follow this behavior . Composites with 1100 Al matrices had significantly higher impact strengths than those with other matrices . Thin-sheet Izod and Charpy , as well as full-size Charpy , impact strength of B/Al increased with more ductile matrices . Similar results are reported in reference 8 . Composites with the strongest and least ductile matrix , 2024 Al , had the lowest impact strengths . The fracture surface became more jagged and irregular with increasing impact strength , and fiber/matrix projection zones of fibers connected by bonded matrix projected out of the fracture surface . Figure 8 compares fracture surfaces of various B/Al composites from reference 8 . Specimens with lower impact strengths had brittle , planar fracture surfaces . Figure 8(a) shows an enlarged view of the 5052-Al-matrix fracture surface , with no fiber/matrix projection zones present . With increasing impact strength the fracture surface became more jagged . For 5.6-mil-diameter-B/1100 Al composites (fig. 8(b)) , some pullout of bare fibers can be seen at the tops of some of the projection zones , but the general jaggedness and projection zone formation is apparent . Figure 8(c) shows that the projection zone effect is more pronounced in higher-impact-strength , 8-mil-diameter-boron specimens .

Figure 9 shows failed full-size Charpy specimens . The low-energy fracture of the 5.6-mil-diameter-B/5052 Al composite (fig. 9(a)) was planar and showed no matrix shear . Restraint by the boron fibers reduced matrix ductility below its unreinforced value . The 2024- , 5052- , and 6061-Al-matrix composites acted in the matrix-less-ductile-than-fibers manner of reference 25 . The ductility of the 1100 Al matrix was high enough so that it was more ductile than the fibers . Higher-energy 5.6-mil-diameter-B/1100 Al composites (fig. 9(b)) show jagged fracture surfaces with large amounts of shear deformation . Figure 10 shows that the shear displacement at the ends of failed LT full-size Charpy specimens increases linearly with increasing impact strength .

In high-impact-strength B/1100 Al composites the matrix sheared after pendulum impact and the fibers failed in tension . With additional shear the tensile stresses in the intact portions of the broken fibers continued to increase and failed the fibers again . This increased the impact strength of the composite in two ways . First , additional energy was absorbed through multiple breakage of the fibers . Second , the matrix absorbed more energy through additional shear after initial fiber fractures .

Effect of Fiber Diameter

Area-compensated LT impact strengths of 1100-Al-matrix composites with various fiber diameters are plotted in figure 5 for three types of impact tests. These results indicate that the impact strength of B/Al increased with increasing boron diameter. Reference 8 also reports that the impact strength of B/1100 Al was higher for specimens with 8-mil-diameter boron fibers than for those with 5.6-mil-diameter B fibers. Limited data in references 7 and 15 show similar results. Work of fracture in copper-matrix composites with brittle, recrystallized tungsten wires also increased with increasing fiber diameter (ref. 16).

For a given fiber content, increasing fiber diameter decreased the total surface-to-volume ratio of the fibers within the composite. Increasing the diameter from 4 mils to 5.6 mils or from 5.6 mils to 8 mils doubled the cross-sectional area of a single fiber, but only increased the shear area by 40 percent. The shear stress would be higher at a given tensile load, if a ductile matrix and/or fiber/matrix interface were allowed to yield and shear prior to composite fracture. Shear is desirable if the matrix has sufficient ductility to allow plastic shear without premature crack initiation prior to fracture.

Interfiber distance must be great enough to allow the matrix to exhibit its full ductility and to absorb impact energy by shear deformation. The increase in effective fiber diameter caused by restraint of the matrix by the fibers (ref. 29) reduces the distance between adjacent fibers for accommodating shear displacement. This effect decreases with increasing fiber diameter, since interfiber distances are correspondingly larger for a given fiber content. Specimens with 4-mil-diameter boron fibers underwent little shear during fracture and had the lowest impact strengths. No multiple fiber breakage was observed, and the ductility of the 1100 Al matrix was minimal. The increase in effective fiber diameter reduced the already small interfiber distance, and the matrix could not act in a ductile manner.

Increasing the boron diameter to 5.6 mils increased the interfiber spacing. These specimens exhibited an increase in fracture ductility and in impact strength. In this case the interfiber spacing was sufficient to allow some shear and multiple fiber breakage to occur.

Composites with 8-mil-diameter boron fibers showed more shear ductility and multiple fiber breakage. Figure 11 shows a failed 8-mil-diameter-B/1100 Al thin-sheet Izod specimen. The outer fibers have a large number of radial cracks in the

fracture region. The cracks are at fairly regular distances along the fiber length. They indicate that multiple fiber breakage occurred prior to and during failure. This fiber breakage was localized in the fracture area. Minimal breakage, similar to that for untested specimens, was observed away from the fracture.

Comparison of figures 8(b) and (c) shows that specimens with 8-mil-diameter boron fibers had much more pronounced fiber/matrix projection zones than specimens with 5.6-mil-diameter boron fibers. This can be attributed to the interfiber distances being large enough that the matrix could achieve sufficient ductility to maximize fracture energy by additional shear and subsequent multiple fiber breakage. The use of 8-mil-diameter boron fibers in composites with other matrices also increased their impact strengths over those previously reported for composites with 4-mil-diameter boron fibers. From these results it can be postulated that the use of even larger diameter boron fibers could further increase the impact strength of composites with 6061 and 5052 Al matrices.

Reference 30 reports Charpy impact results on boron-, carbon-, or glass-fiber composites with resin matrices of various toughnesses. Calculations were made to determine the relative contribution of fiber pullout, shear delamination, and fiber fracture energies. Two-thirds of the calculated energy came from the energy absorbed by fiber fracturing, which was in turn proportional to the area under the stress-strain curve of the fiber. Glass fibers, having much higher strengths and failure strains, had the largest area under the stress-strain curve and gave the highest Charpy impact strengths. Boron fibers were next; and carbon fibers, with the lowest strain and area under the curve, had the lowest impact results. Furthermore, the impact strength was independent of the toughness of the matrices, because of the overpowering influence of the fibers.

These results are significant because they show that, in a brittle matrix composite, the major energy-absorbing contribution comes from fiber fracturing. Composite impact properties are an interaction of the energy contributions of all the constituents in the composite: the matrix, the fiber, and the interface. However, the strain and the impact behavior of each component are interrelated and must be such that the full contribution from each can be attained. A brittle resin matrix does not contribute much to the energy-absorbing capability of a composite. A ductile matrix, such as 1100 Al, can make a significant contribution to the overall impact energy by allowing additional energy absorption through matrix shear as well as through

fiber fracture. Thus, where possible, it is vitally important to have a matrix with sufficient ductility to allow the fibers to approach their full strength and strain capability.

Effect of Directionality

While most of the preceding discussion has been concerned with LT impact testing, anisotropy in both LT and TT impact was observed. In these tests the 1100 Al matrix does not exhibit the energy-absorbing shear ductility shown in the LT tests. In unidirectional B/Al composites the fibers must be broken during LT failure, but in TT failure the fracture path extends primarily through the unreinforced matrix and around the fibers without necessarily breaking or splitting them.

Figure 12 shows the transverse fracture zone of failed thin-sheet Charpy specimens. The fracture crack split a few of the fibers in composites with 4- and 5.6-mil-diameter boron fibers in 1100 Al (figs. 12(b) and (c)). The 8-mil-diameter-B/1100 Al composites show very little fiber splitting (fig. 12(a)). However, in 8-mil-diameter-B/2024 Al composites every fiber in the fracture plane appeared to be split (fig. 12(d)). This difference in splitting behavior can be attributed to the increased strength of the 2024 Al matrix and to the stronger B/Al bond formed at the higher fabrication temperatures used to process the 2024 Al composites. It also appears that the transverse strength of the 8-mil-diameter boron fibers was less than that of the 2024 Al matrix; thus, the fracture path followed the plane of weakness. In 1100 Al composites the transverse strengths of the fiber and the interface were nearly equal, and the fracture path appeared to be random, preferring to go through the matrix but occasionally splitting the fibers.

An unexpected directionality effect reported in reference 8 was the reduced impact strength observed in full-size Charpy tests in the LT(s) direction. The impact strength of specimens of LT(s) geometry dropped as much as 30 to 50 percent below that of the LT specimens. Figure 13 shows failed 8-mil-diameter-B/1100 Al LT and LT(s) specimens. The LT specimens had much larger shear deformation than the LT(s) specimens. Fracture surfaces of high-energy LT specimens (fig. 8(c)) show massive fiber/matrix projection zones. The LT(s) specimens show less fiber/matrix projection zone formation (fig. 14). The fibers are aligned in intact vertical planes and appear to show evidence of bare-fiber pull out. The vertical planes are from

the individual-ply layup during consolidation. In this case the crack propagation direction is normal to the edge of the ply, and the fracture crack proceeds throughout all the plies simultaneously. The spread area shown on the figure is a result of tup impact.

In diffusion bonding, fiber layers are placed between matrix foils and consolidated. Upon impact testing of LT specimens, the crack must propagate sequentially through fully dense aluminum foils with weaker Al/Al interfaces separating the individual foils. For LT(s) specimens, the crack must propagate simultaneously across the entire number of plies acting as a unit.

If bonding were not perfect, the strength of the foils would be greater in the fully dense direction of the plane of the foil than in the direction where the foils were bonded to each other. Each B/Al ply is fully dense and well bonded and tends to act as a laminate unit. The planes of weakness in a B/1100 Al composite are at the Al/Al and B/Al interfaces. Thus, in a notched full-size Charpy test, the notch effect is negated immediately below the notch tip by delamination at the first ply. After initial delamination the specimen bends by shear and acts in a ductile manner resulting in high impact energies. In LT(s) specimens, delamination and/or sufficient shear deformation to blunt the crack does not occur. Instead of having uniform plies to deform by shear, LT(s) specimens must fracture simultaneously through a number of plies. None of these plies are oriented preferentially for shear, and thus the fibers are not permitted to exhibit their maximum strain capability. Therefore, the impact strength of LT(s) specimens is reduced to a value approaching that of a restrained, nonductile matrix.

SUMMARY OF RESULTS AND CONCLUSIONS

The following results and conclusions were obtained from studies to improve the impact properties of diffusion-bonded boron/aluminum (B/Al) composites:

1. Impact strength of B/Al can be improved by proper choice of fabrication temperature. Processing at below-optimum temperatures caused impact strength to be reduced by fiber/matrix interface delamination. Above the optimum temperature, impact strength was reduced by excessive reaction at the fiber/matrix interface and by the formation of bond strengths in excess of those required for best impact performance.

2. The impact strength of B/1100-Al-matrix composites was significantly higher than that of composites with 2024, 5052, or 6061 Al matrices. More ductile matrices allowed additional energy absorption through matrix shear deformation and multiple fiber breakage.

3. Larger diameter boron fibers increased impact strength. They provided larger interfiber spacing, allowing the matrix to act in a more ductile manner and permitting the fibers to attain a greater portion of their full strength and strain capability.

4. the LT(s) impact strength (notched side parallel to pressing direction) was lower than the LT impact strength (notched side normal to pressing direction.)

5. Thin-sheet Izod and Charpy impact tests can be used for ranking purposes to compare impact properties with those obtained from full-size Charpy tests, but the quantitative results of one type of test cannot be extrapolated to another.

Lewis Research Center,
National Aeronautics and Space Administration,
Cleveland, Ohio, May 4, 1976,
505-01.

REFERENCES

1. Metal-Matrix Composites: Status and Prospects. (NMAB-313, Natl. Mat. Advisory Board; Contract MDA903-74-C-0167), NASA CR-142191, 1974.
2. Signorelli, Robert A.: Metal Matrix Composites for Aircraft Propulsion Systems. NASA TM X-71685, 1975.
3. Norbut, T. J.: Fatigue Tolerance of Damaged Metal Composite Blading. Impact of Composite Materials on Aerospace Vehicles and Propulsion Systems. AGARD-CP-112, Advisory Group for Aerospace Research and Development (France), 1973.
4. DeJong, A. P.: Their Airspace or Ours? Shell Aviation News, no. 290, 1970, pp. 2-7.
5. Metals Handbook. Am. Soc. Metals, 1948, p. 212.

6. Kreider, Kenneth G.; Dardi, L.; and Prewo, K.: Metal Matrix Composite Technology. K910853-12, United Aircraft Corp. (AD-740584; AFML-TR-71-204), 1971.
7. Dardi, L. E.; and Kreider, K. G.: The Notched Impact and Flexural Behavior of Boron-Aluminum. Failure Modes in Composites. Istvan Toth, ed., Am. Inst. Mining, Metall. and Petroleum Engrs., 1973, pp. 231-270.
8. Melnyk, P.; and Toth, I. J.: Development of Impact Resistant Boron/Aluminum Composites for Turbojet Engine Fan Blades. (ER-7806, TRW Equipment Labs.; NAS3-17763), NASA CR-134770, 1975.
9. Winsa, Edward A.; and Petrasek, Donald W.: Factors Affecting Miniature Izod Impact Strength of Tungsten-Fiber - Metal Matrix Composites. NASA TN D-7393, 1973.
10. Standard Methods for Notched Bar Impact Testing of Metallic Materials. 1967 Book of ASTM Standards, Pt. 31, Designation E23-66, Am. Soc. Testing Mater., 1967, pp. 284-300.
11. Operating Instructions for Magnatest Elastomat Type FM-500. Magnaflux Corp., 1960.
12. Forster, F.: Ein neues Messverfahren zur Bestimmung des Elastizitätsmoduls und der Dämpfung. (A New Method of Measurement of Elastic Modulus and Damping.) Z. für Metallkunde, vol. 29, 1937, pp. 109-115.
13. McDanel, David L.; and Signorelli, Robert A.: Effect of Angleply and Matrix Enhancement on Impact-Resistant Boron/Aluminum Composites. NASA TN D-8205, 1976.
14. Wilshaw, T. R.; and Pratt, P. L.: On the Plastic Deformation of Charpy Specimens Prior to General Yield. J. Mech. Phys. Solids, vol. 14, 1966, pp. 7-19.
15. Hoover, W. R.; and Allred, R. E.: The Toughness of Borsic-Al Composites with Weak Fiber-Metal Bonds. SC-DC-714467, Sandia Labs., 1972.
16. Cooper, G. A.; and Kelly, A.: Tensile Properties of Fibre-Reinforced Metals: Fracture Mechanics. J. Mech. Phys. Solids, vol. 15, 1967, pp. 279-297.

17. Hancock, J. R.; and Swanson, G. D.: Toughness of Filamentary Boron/Aluminum Composites. Composite Materials: Testing and Design (Second Conference). ASTM STP-497, Am. Soc. Testing Mater., 1972, pp. 299-310.
18. Phillips, D. C.: The Fracture Energy of Carbon-Fibre Reinforced Glass. J. Mater. Sci., vol. 7, no. 10, Oct. 1972, pp. 1175-1191.
19. Chamis, Christos C.; Hanson, Morgan P.; and Serafini, Tito T.: Designing for Impact Resistance with Unidirectional Fiber Composites. NASA TN D-6463, 1971.
20. Piggott, M. R.: The Effect of Aspect Ratio on Toughness in Composites. J. Mech. Phys. Solids, vol. 9, 1974, pp. 494-502.
21. Kelly, A.: Interface Effects and the Work of Fracture of a Fibrous Composite. Proc. Roy. Soc. (London), vol. 319A, no. 1536, Oct. 1970, pp. 95-116.
22. Hancock, J. R.; and Shaw, G. G.: Effect of Filament-Matrix Interdiffusion on the Fatigue Resistance of Boron-Aluminum Composites. Composite Materials: Testing and Design (Third Conference). ASTM STP-546, Am. Soc. Testing Mater., 1974, pp. 497-506.
23. Prewo, Karl A.: The Charpy Impact Energy of Boron-Aluminum. J. Comp. Mater., vol. 6, 1972, pp. 442-455.
24. Hoover, W. R.; and Allred, R. E.: The Dynamic Fracture Behavior of Borsic-Al Composites. SC-DC-721080, Sandia Labs., 1972.
25. Cooper, G. A.; and Kelly, A.: Role of the Interface in the Fracture of Fiber-Composite Materials. Interfaces in Composites. ASTM STP-452, Am. Soc. Testing Mater., 1969, pp. 90-106.
26. Cooper, G. A.: The Fracture Toughness of Composites Reinforced with Weakened Fibres. J. Mater. Sci., vol. 5, no. 8, Aug. 1970, pp. 645-654.
27. Harris, Bryan: The Strength of Fibre Composites. Composites, vol. 3, no. 4, July 1972, pp. 152-167.
28. Helfet, J. L.; and Harris, B.: Fracture Toughness of Composites Reinforced with Discontinuous Fibres. J. Mater. Sci., vol. 7, no. 5, May 1972, pp. 494-498.

29. Jech, Robert W.; and Signorelli, Robert A.: The Effect of Interfiber Distance and Temperature on the Critical Aspect Ratio in Composites. NASA TN D-4548, 1968.
30. Novak, R. C.; and DeCrescente, M. A.: Impact Behavior of Unidirectional Resin Matrix Composites Tested in the Fiber Direction. Composite Materials: Testing and Design (Second Conference). ASTM STP-497, Am. Soc. Testing Mater., 1972, pp. 311-323.

TABLE I. - MECHANICAL PROPERTIES OF ALUMINUM-MATRIX ALLOYS

[Modified from ref. 5.]

Alloy	Yield strength		Tensile strength		Elongation, percent	Impact strength		Type of test
	MPa	ksi	MPa	ksi		J	ft-lb	
1100	28	4	90	13	42	26	19	Izod
2024	303	44	455	66	23	18	13	Charpy
5052	179	26	221	32	14	79	58	Charpy
6061	55	8	124	18	22	--	--	-----

TABLE II. - RESULTS OF UNNOTCHED THIN-SHEET IZOD

IMPACT SCREENING TESTS

[Fiber, unidirectional 0.20-mm-(8-mil-) diameter boron; matrix, 1100 aluminum; tested at room temperature.]

Fabrication conditions		Time, hr	Impact energy		Area-compensated impact strength		Type of failure
Temperature	K		°F	J	in-lb	kJ/m ²	
Longitudinal							
714	825	0.5	0.81	7.2	69.7	33.2	Delamination
			1.20	10.6	87.4	41.6	Delamination
			.76	6.7	55.1	26.3	Delamination
728	850	0.5	2.08	18.4	164.3	78.2	Fibrous
			1.46	12.9	113.2	53.9	Delamination
			1.07	9.5	81.3	38.7	Delamination
			1.04	9.2	77.7	37.0	Delamination
728	850	1.0	0.84	7.4	46.6	22.2	Delamination
			.70	6.2	42.0	20.0	Delamination
			1.48	13.1	90.1	42.9	Fibrous
742	875	1.0	1.21	10.7	100.8	48.0	Fibrous
			1.75	15.5	138.0	65.5	Fibrous
			1.57	13.9	131.1	62.4	Fibrous
755	900	0.5	2.28	20.2	149.5	71.1	Fibrous
			2.11	18.7	142.0	67.6	Fibrous
			1.16	10.3	99.7	47.5	Fibrous
			1.41	12.5	115.9	55.2	Delamination
			1.57	13.9	104.9	49.9	Delamination
783	950	0.5	1.48	13.1	112.0	53.3	Fibrous
			1.43	12.7	107.7	51.2	Fibrous
			1.47	13.0	113.2	53.9	Fibrous
Transverse							
728	850	1.0	0.06	0.5	4.3	2.0	Separation
742	875	1.0	0.09	0.8	6.8	3.2	Separation
			.09	.8	6.8	3.2	Separation
755	900	0.5	0.06	0.5	3.9	1.8	Separation
			.07	.6	4.6	2.2	Separation
783	950	0.5	0.18	1.6	13.3	6.3	Separation
			.09	.8	6.8	3.7	Separation

TABLE III. - RESULTS OF DYNAMIC MODULUS-
OF-ELASTICITY TESTS

[Fiber, unidirectional boron tested at room
temperature.]

Matrix	Fiber diameter		Modulus of elasticity			
			Longitudinal		Transverse	
	mm	mils	GPa	Mpsi	GPa	Mpsi
1100 Al	0.20	8.0	218	31.6	130	18.8
			219	31.8	131	19.0
1100 Al	0.10	4.0	219	31.7	114	16.6
			221	32.1	122	17.6
1100 Al	0.14	5.6	221	32.0	129	18.7
			224	32.5	124	18.0
2024 Al	0.20	8.0	223	32.3	128	18.5
			225	32.6	129	18.7
5052 Al	0.20	8.0	211	30.5	108	15.6
			207	30.1	104	15.0
6061 Al	0.20	8.0	214	31.0	116	16.9
			210	30.5	111	16.1

TABLE IV. - RESULTS OF TENSILE TESTS

[Fiber, unidirectional boron tested at room
temperature.]

Matrix	Fiber diameter		Ultimate tensile strength			
			Longitudinal		Transverse	
	mm	mils	MPa	ksi	MPa	ksi
1100 Al	0.20	8.0	1175	170.4	32	4.7
			1296	188.0	---	----
1100 Al	0.10	4.0	1495	216.9	---	----
1100 Al	0.14	5.6	1513	219.4	39	5.6
2024 Al	0.20	8.0	981	142.3	101	14.7
			959	139.1	---	----
5052 Al	0.20	8.0	1225	177.7	99	14.3
			1160	168.3	---	----
6061 Al	0.20	8.0	1703	246.9	71	10.3

TABLE V. - RESULTS OF UNNOTCHED THIN-SHEET IZOD IMPACT TESTS

[Fiber, unidirectional boron tested at room temperature.]

Matrix	Fiber diameter		Longitudinal				Transverse			
	mm	mils	Impact energy		Area-compensated impact strength		Impact energy,		Area-compensated impact strength	
			J	ft-lb	kJ/m ²	ft-lb/in ²	J	ft-lb	kJ/m ²	ft-lb/in ²
1100 Al	0.20	8.0	2.98	2.42	223	106.1	0.19	0.14	13	6.0
			2.89	2.13	210	100.1	----	----	--	---
			2.28	1.68	166	78.9	----	----	--	---
			2.25	1.66	169	80.6	----	----	--	---
			>3.00	>2.21	>216	>102.8	----	----	--	---
1100 Al	0.10	4.0	0.60	0.44	71	33.8	0.04	0.03	6	2.7
			.66	.49	80	38.2	.05	.04	7	3.5
			.57	.42	73	34.5	----	----	--	---
1100 Al	0.14	5.6	1.02	0.75	99	46.9	0.04	0.03	4	2.1
			.91	.67	88	41.8	.05	.04	6	2.9
			.89	.66	90	42.8	----	----	--	---
2024 Al	0.20	8.0	0.51	0.38	37	17.4	0.11	0.08	8	4.0
			.45	.33	35	16.7	.15	.11	12	5.6
5052 Al	0.20	8.0	0.88	0.65	65	31.0	0.22	0.16	15	7.1
			.84	.62	61	29.1	.20	.15	14	6.8
6061 Al	0.20	8.0	0.73	0.54	56	26.6	0.19	0.14	13	6.3
			.65	.48	46	21.9	.24	.18	17	7.9

TABLE VI. - RESULTS OF UNNOTCHED THIN-SHEET CHARPY IMPACT TESTS

[Fiber, unidirectional boron tested at room temperature.]

Matrix	Fiber diameter		Longitudinal				Transverse			
	mm	mils	Impact energy		Area-compensated impact strength		Impact energy		Area-compensated impact strength	
			J	ft-lb	kJ/m^2	ft-lb/in^2	J	ft-lb	kJ/m^2	ft-lb/in^2
1100 Al	0.20	8.0	6.13	4.52	327	155.7	0.53	0.39	27	12.8
			4.99	3.68	256	121.7	----	----	--	----
			3.89	2.87	193	91.9	----	----	--	----
			4.01	2.96	198	94.2	----	----	--	----
1100 Al	0.10	4.0	1.19	0.88	107	51.0	0.20	0.15	18	8.5
			.99	.73	88	42.0	----	----	--	----
1100 Al	0.14	5.6	1.50	1.11	107	50.7	0.18	0.13	13	6.0
			2.36	1.74	167	79.3	----	----	--	----
2024 Al	0.20	8.0	0.77	0.57	44	20.8	0.31	0.23	17	8.1
			.75	.55	42	20.1	----	----	--	----
5052 Al	0.20	8.0	1.67	1.23	84	40.0	0.85	0.63	43	20.5
			1.88	1.39	95	45.1	----	----	--	----
6061 Al	0.20	8.0	1.59	1.17	80	38.3	0.27	0.24	16	7.5
			1.53	1.13	77	36.8	----	----	--	----

TABLE VII. - RESULTS OF NOTCHED FULL-SIZE CHARPY IMPACT TESTS

[Fiber, unidirectional boron tested at room temperature.]

Matrix	Fiber diameter		Test type		Impact strength		Area-compensated impact strength	
			Geometry	Source	J	ft-lb	kJ/m ²	ft-lb/in ²
	mm	mils						
1100 Al	0.20	8.0	LT	Lewis	^a 24.4	^a 18.0	^a 302	^a 144
					^a 25.1	^a 18.5	^a 311	^a 148
					^a 17.6	^a 13.0	^a 218	^a 104
				Ref. 8	96.3	71.0	1193	568
			91.6		67.5	1134	540	
			LT(s)	Lewis	35.9	26.5	445	212
Ref. 8	47.5	35.0		588	280			
1100 Al	0.10	4.0	LT	Lewis	38.0	28.0	470	224
					29.8	22.0	370	176
1100 Al	0.14	5.6	LT	Lewis	51.5	38.0	638	304
					42.0	31.0	521	248
					Ref. 8	63.7	47.0	790
				Ref. 8	46.8	34.5	580	276
			LT(s)	Ref. 8	28.5	21.0	353	168
2024 Al	0.20	8.0	LT	Lewis	9.5	7.0	118	56
5052 Al	0.20	8.0	LT	Lewis	13.6	10.0	168	80
				Ref. 8	16.5	11.0	185	88
					13.6	10.0	168	80
6061 Al	0.20	8.0	LT	Lewis	10.2	7.5	126	60

^aPoorly bonded specimen; delaminated during testing; data not plotted in figures.

TABLE VIII. - IMPACT FRACTURE MODES IN
BORON/ALUMINUM COMPOSITES

Fracture mode	Energy-absorption contribution			
	Total	Fiber	Matrix	Interface
Cleavage	Very low	Very low	Very low	Very low
Planar	Low	Low	Low	Low
Delamination	Medium	Low	Low	Medium
Pullout	Medium	Low	Medium	Low
Matrix shear (single fiber failure)	High	High	High	High
Matrix shear (multiple fiber failure)	Very high	Very high	Very high	Very high

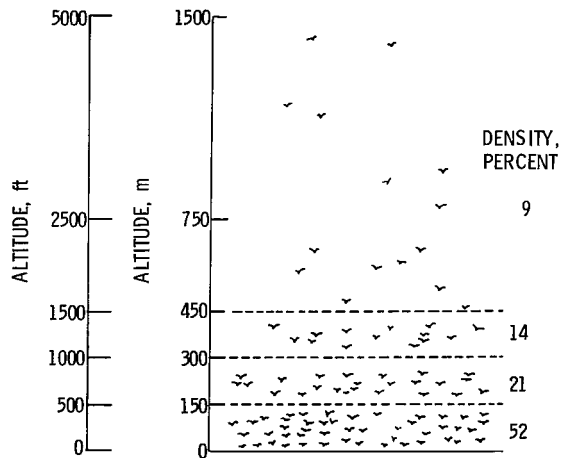


Figure 1. - Average density of local bird population with altitude (ref. 3).

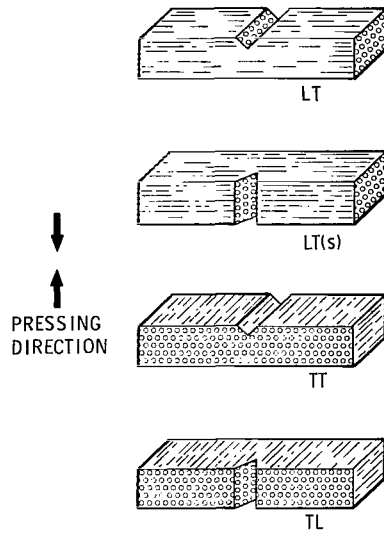
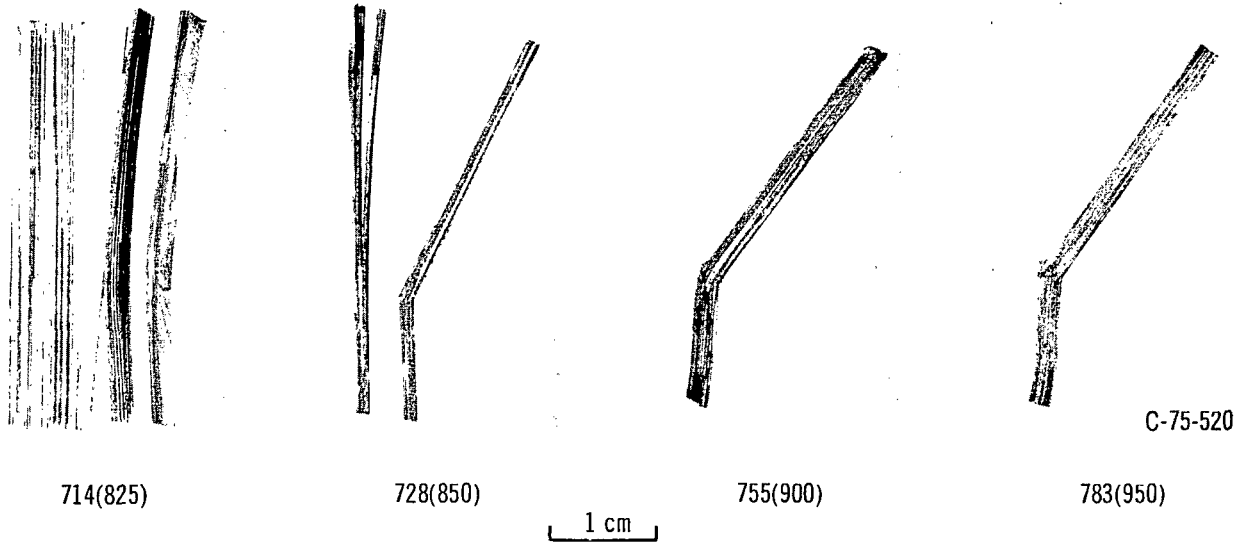


Figure 2. - Charpy impact test specimen geometries.



Bonding temperature, K(°F):

714(825)

728(850)

755(900)

783(950)

1 cm

Figure 3. - Failed thin-sheet Izod specimens from fabrication-condition screening tests. Bonding time, 0.5 hour; fiber, 8-mil-diameter boron; matrix, 1100 aluminum.



Figure 4. - Impact delamination failure at boron/aluminum interface. X30.

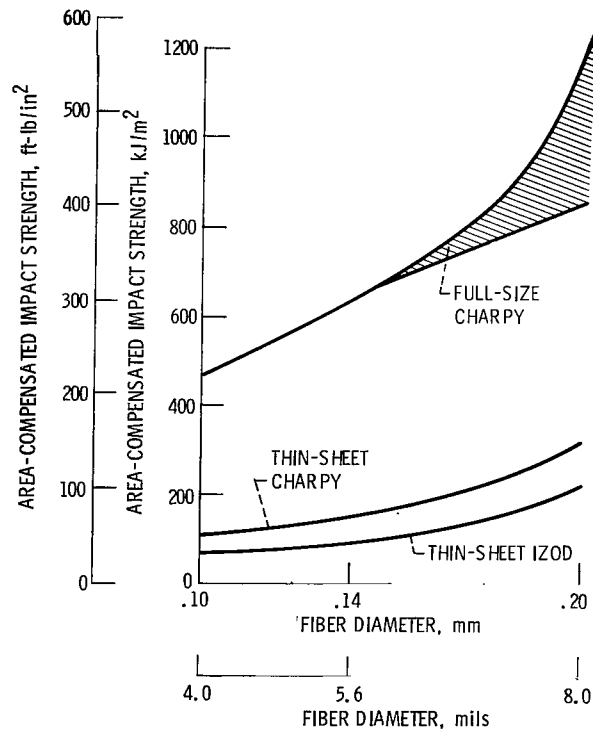


Figure 5. - Area-compensated longitudinal impact strengths of unidirectional 1100 aluminum composites from different types of impact tests.

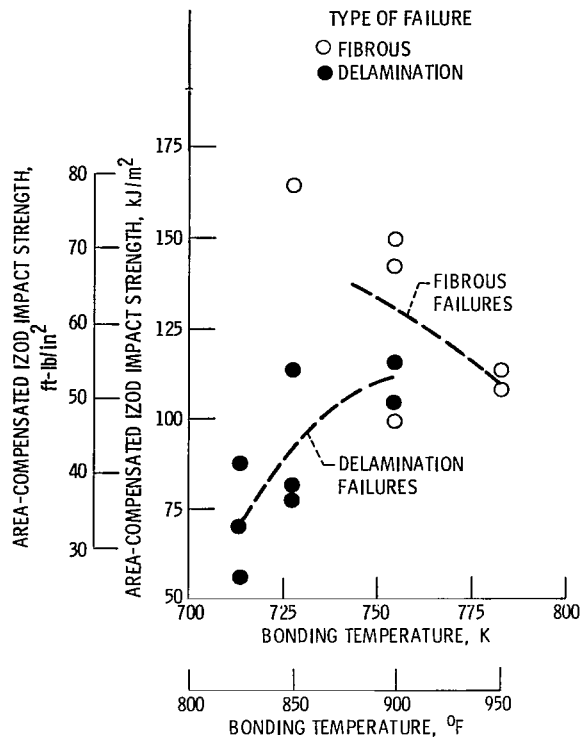


Figure 6. - Effect of bonding temperature on area-compensated thin-sheet longitudinal Izod impact strength of 8-mil-diameter B/1100 Al composites. Bonding time, 0.5 hour.

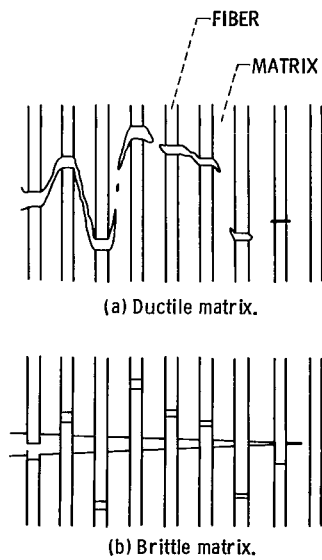
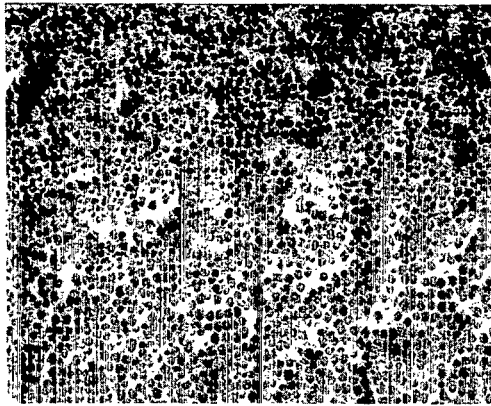
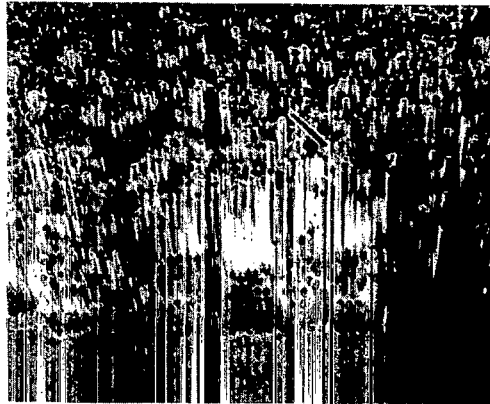


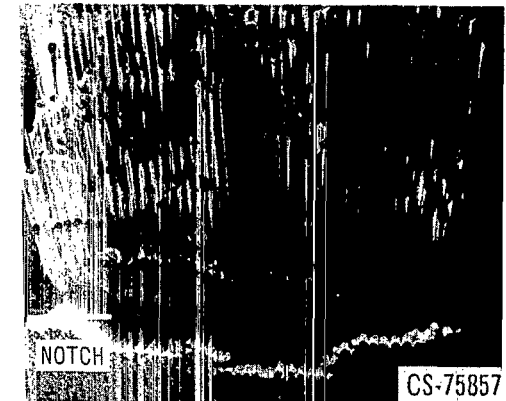
Figure 7. - Crack propagation in composites with matrices of different ductilities. (From ref. 25.)



(a) 5.6-Mil-diameter-B/5052 Al. X10.

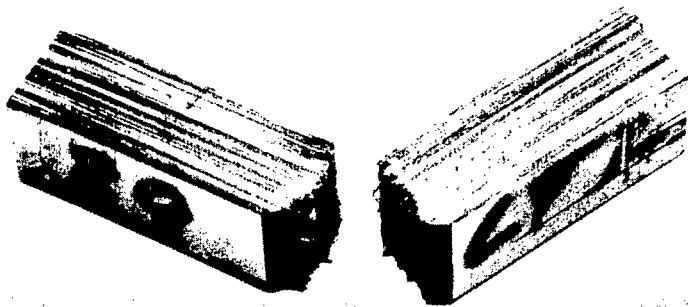


(b) 5.6-Mil-diameter-B/1100 Al. X10.

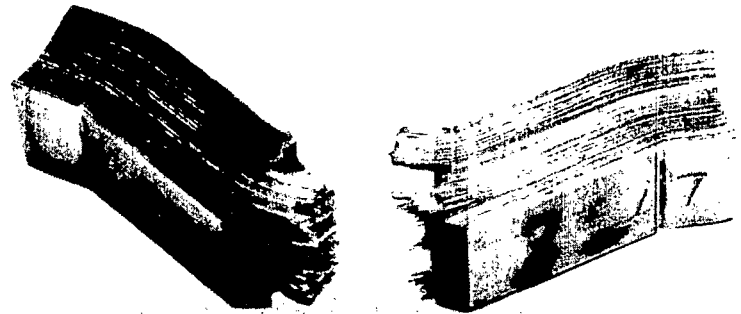


(c) 8-Mil-diameter-B/1100 Al. X6.

Figure 8. - Failed full-size LT Charpy impact test specimens showing effect of various matrices and fiber diameters on projection zones in boron/aluminum composites. (From ref. 8.)



(a) 5.6-Mil-diameter-B/5052 Al; impact strength, 18 J (13 ft-lb).



(b) 5.6-Mil-diameter-B/1100 Al; impact strength, 64 J (47 ft-lb).



(c) 8-Mil-diameter-B/1100 Al; impact strength, 96 J (71 ft-lb).

Figure 9. - Failed full-size unidirectional LT Charpy impact test specimens. (From ref. 8.)

CS-73473

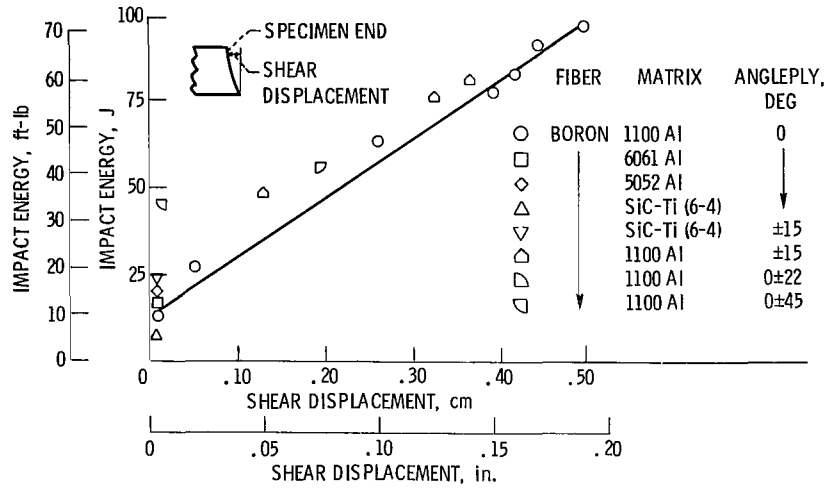
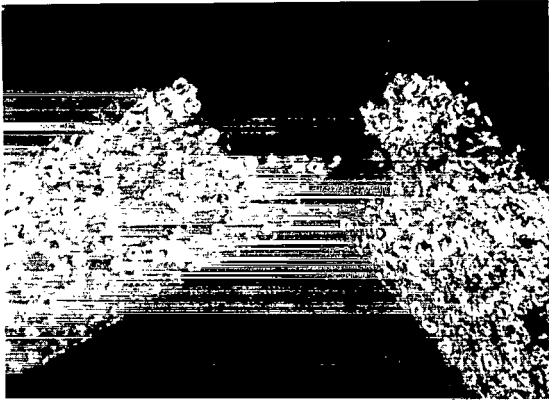


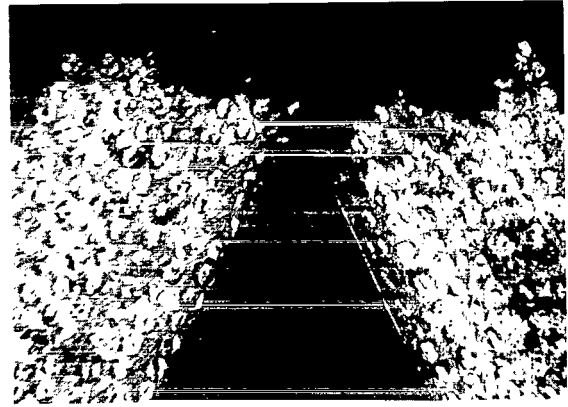
Figure 10. - Shear displacement at the ends of various failed full-size LT Charpy impact test specimens. (From ref. 8.)



Figure 11. - Fracture region of failed unidirectional 8-mil-diameter-B/1100 Al thin-sheet Izod impact test specimen showing multiple fiber breakage. X32.



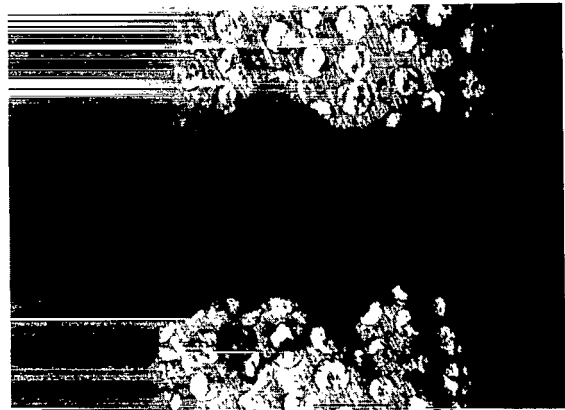
(a) 4-Mil-diameter-B/1100 Al.



(b) 5.6-Mil-diameter-B/1100 Al.



(c) 8-Mil-diameter-B/1100 Al.



(d) 8-Mil-diameter-B/2024 Al.

Figure 12. - Fracture surfaces of failed TT thin-sheet Charpy impact test specimens. X35.



(a) LT; impact strength, 96.5 J (71 ft-lb).



(b) LT(s); impact strength, 47.5 J (35 ft-lb).



CS-75855

Figure 13. - Failed 8-mil-diameter-B/1100 Al full-size LT and LT(s) Charpy impact test specimens. (From ref. 8.)

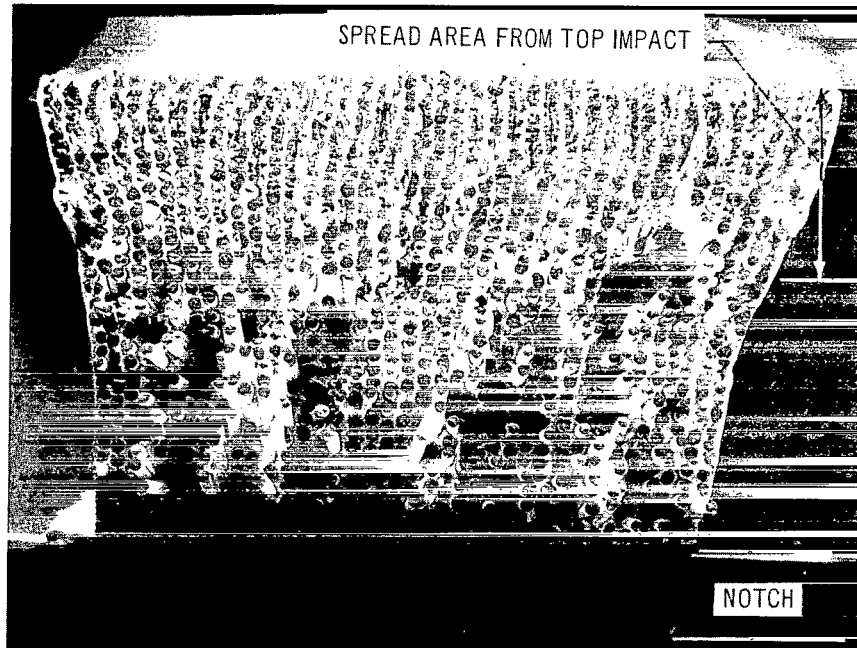


Figure 14. - Fracture surface of failed 8-mil-diameter-B/1100 Al full-size LT(s) test specimen. Impact strength, 47.5 J (35 ft-lb). (From ref. 8.)



868 001 C1 U C 761029 S00903DS
DEPT OF THE AIR FORCE
AF WEAPONS LABORATORY
ATTN: TECHNICAL LIBRARY (SUL)
KIRTLAND AFB NM 87117

POSTMASTER: If Undeliverable (Section 158
Postal Manual) Do Not Return

"The aeronautical and space activities of the United States shall be conducted so as to contribute to the expansion of human knowledge of phenomena in the atmosphere and space. The Administration shall provide for the widest practicable and appropriate dissemination of information concerning its activities and the results thereof."

—NATIONAL AERONAUTICS AND SPACE ACT OF 1958

NASA SCIENTIFIC AND TECHNICAL PUBLICATIONS

TECHNICAL REPORTS: Scientific and technical information considered important, complete, and a lasting contribution to existing knowledge.

TECHNICAL NOTES: Information less broad in scope but nevertheless of importance as a contribution to existing knowledge.

TECHNICAL MEMORANDUMS: Information receiving limited distribution because of preliminary data, security classification, or other reasons. Also includes conference proceedings with either limited or unlimited distribution.

CONTRACTOR REPORTS: Scientific and technical information generated under a NASA contract or grant and considered an important contribution to existing knowledge.

TECHNICAL TRANSLATIONS: Information published in a foreign language considered to merit NASA distribution in English.

SPECIAL PUBLICATIONS: Information derived from or of value to NASA activities. Publications include final reports of major projects, monographs, data compilations, handbooks, sourcebooks, and special bibliographies.

TECHNOLOGY UTILIZATION PUBLICATIONS: Information on technology used by NASA that may be of particular interest in commercial and other non-aerospace applications. Publications include Tech Briefs, Technology Utilization Reports and Technology Surveys.

Details on the availability of these publications may be obtained from:

SCIENTIFIC AND TECHNICAL INFORMATION OFFICE

NATIONAL AERONAUTICS AND SPACE ADMINISTRATION
Washington, D.C. 20546